



## SUPERPLASTIC BEHAVIOR OF 2024 ALUMINUM ALLOY SHEET SUBJECTED TO THERMOMECHANICAL PROCESSING

Luciana RUS, Marius TINTELECAN, Monica SAS-BOCA,  
Dan NOVEANU, Ionut MARIAN

Technical University of Cluj-Napoca  
email: [Luciana.Rus@ipm.utcluj.ro](mailto:Luciana.Rus@ipm.utcluj.ro)

### ABSTRACT

*This paper describes the superplastic behavior of the commercial 2024 aluminum alloy. The investigated alloy was processed in a 3 mm thick sheet form. The superplastic properties of the alloy were investigated using an uniaxial tensile testing, with a constant strain rate in the range  $8 \times 10^{-4} \div 1 \times 10^{-2} \text{ s}^{-1}$ , at temperatures in the range  $450 \div 480^\circ\text{C}$ . The investigations included the determination of the true-strain, the true-stress characteristics, the elongation to failure, the strain-rate sensitivity exponent  $m$  and the aspect of the alloy microstructure. Elongations to failure longer than 200% for the fine grained 2024 aluminum alloy were obtained at  $460^\circ$  and lower strain rates and at  $480^\circ\text{C}$  and a higher strain rate.*

KEYWORDS: 2024 aluminum alloy, elongation to failure, strain-rate sensitivity exponent, superplastic properties, thermomechanical processing

### 1. Introduction

The attractive characteristics of aluminum alloys have become of great interest both in the academic and in the industrial research fields. Their high specific strength can be functional for most of the structural purposes. The exceptional elongation can be reached only by the grain refinement technique: powder-metallurgy processing, thermomechanical processing, severe plastic deformation [1]. One method to produce a very fine grain size usually consists of rolling and then carrying out a heat treatment which causes a precipitation of another phase or phases in a finely divided form, pins at the grain boundaries of the simultaneously recrystallizing matrix [2]. This is the technique used for producing commercial superplastic aluminum alloys.

However, the basic requirement of fine grain size ( $<10 \mu\text{m}$ ) is a necessary but not always a sufficient condition to obtain superplasticity [3]. If the fine grain microstructure is not stable at high temperatures, superplastic elongation will be significantly reduced.

Superplasticity is defined as the ability of a polycrystalline material to exhibit, in a generally isotropic manner, very high tensile elongations prior to failure [4]. There are two basic requirements for achieving superplasticity: first, a very small and stable grain size, typically less than  $\sim 10 \mu\text{m}$ ; second, a high testing temperature, typically  $\geq 0,5 T_m$  (where  $T_m$

represents the absolute melting temperature of the material), so that diffusion-controlled processes are reasonably rapid. Superplastic elongations are achieved over a limited range of strain rate in the superplastic region II ( $10^{-5} \div 10^{-3} \text{ s}^{-1}$ ) [5, 6].

### 2. Material and experimental procedure

The material studied in this work is an extruded bar (22 mm in diameter) of commercial aluminum alloy 2024-T3, produced by S.C. ALPROM S.A. Slatina, Romania, with the following chemical composition (in wt %): 4.955 Cu; 1.322 Mg; 0.437 Mn; 0.358 Zn; 0.300 Fe; 0.119 Si; 0.017 Cr; 0.005 Sn; 0.005 Sb; 0.005 Pb; 0.003 Ni; Al-balance.

Because the ductility of the received 2024 aluminum alloy samples is small (tensile tested at temperatures and strain rates used in this research, the tensile elongation is smaller than 108% for round samples of 25 mm gauge length and 5 mm diameter) [7], the material was processed thermomechanically (a method meant to increase the ductility through grain refinement).

The processing route for the 2024 aluminum alloy is shown in Figure 1. The specimens from the received material (60 mm length and 22 mm diameter) were homogenized at  $500^\circ\text{C}$  for 8 hours before rolling. Hot rolling was carried out unidirectionally to obtain a thickness reduction of 68% and prepare a 7 mm thick strip which was

quenched. Then the samples were cold rolled (a final 3 mm thickness, with a thickness reduction of 57%), fast heated up to 480°C, soaked for 15 minutes and

quenched in water. The rolled plates were then soaked at 350°C for 30 minutes, in order to make the fine-grained structure stable.

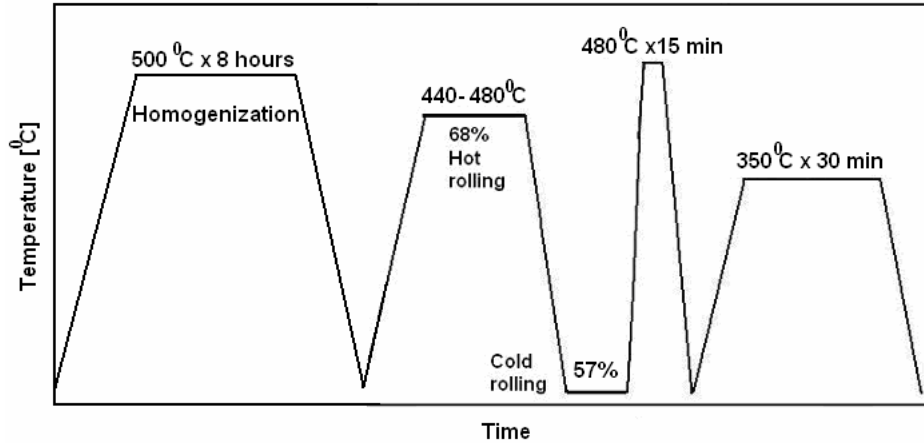


**Fig. 1.** Schematic thermomechanical processing route for 2024 aluminum alloy.

The tensile samples were prepared with a 25 mm gauge length, 6.6 mm width and 3 mm thickness, all of them being machined with the tensile stress direction parallel to the rolling direction.

The tensile tests were conducted on the testing equipment that was interfaced with a computer to provide complete control of the strain rate. After heating the specimens in the electrical horizontal furnace (Carbolite CTF 12/75/700) to the necessary temperatures, for 25÷30 minutes, each specimen was submitted to a tensile axial load which produced the deformation until fracture. The tensile load and the elongation were recorded simultaneously.

Constant strain rate tests were conducted over a range of strain rates of  $8 \times 10^{-4} \div 5 \times 10^{-3} \text{ s}^{-1}$  and test temperatures of 450÷480°C. After fracture the samples were cooled in water to keep the resulting structure during the test. The behavior of the material is described by the constitutive equation [3]  $\sigma = K \dot{\epsilon}^m$  (1), where  $\sigma$  is the true flow stress, K is a constant,  $\dot{\epsilon}$  is the true strain rate and m is the strain rate sensitivity exponent.

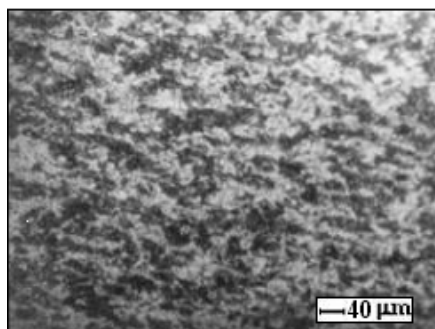
The logarithms equation (1) to obtain a relationship with the general form  $\ln \sigma_i = \ln K + m \ln \dot{\epsilon}_i$  (2), where  $i = 1 \dots N$  representing the number of experimental tests.

The characteristics of the material, m and K, are determined by minimizing the function f (m, lnk) expressed according to the method of least squares, calculating first order derivatives of function f and solving the system of equations [7]. The as-received and as-processed aluminum samples were cut in transversally, polydol mounted, and mechanically polished. Keller's reagent (a composition of 3 ml HCl, 2 ml HF, 5 ml HNO<sub>3</sub> and 190 ml of distilled water) was used to reveal the microstructure of this material by the intercept method.

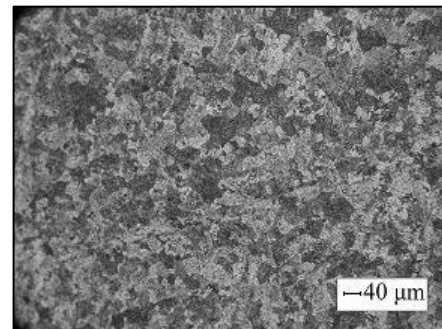
### 3. Experimental results

#### 3.1. Microstructural characteristics

Figure 2 shows the as-received alloy and the microstructural changes during the thermomechanical processing of 2024 aluminum alloy.



a)



b)

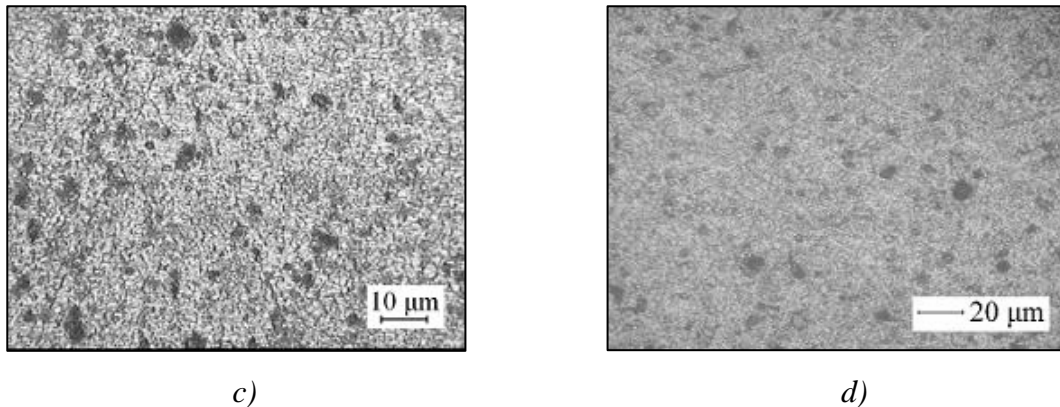


**Fig. 2.** Optical micrographs of 2024 aluminum alloy: a) as-received; b) homogenizing sample; c) hot and cold rolled sample; d) recrystallized sample.

The microstructure of the as-received alloy (figure 2.a) shows a structure consisting in supersaturated in Cu and Mg solid solution, with large grains of 36  $\mu\text{m}$  average size. It is obvious that the chemical composition of the alloy is non-homogeneous and it is necessary to make a homogenization thermal treatment before rolling, by means of which a recrystallized structure is obtained [Figure 2.b)]. During the heating, the soluble components (as  $\text{CuAl}_2$ ) undergo in solid solution and, as a result of diffusion, the equalization of alloying compounds concentration take place at the grain boundaries. During the cooling that follows, the solid solution is decomposed and chemical compounds are separated, refined and uniformly distributed in the alloy matrix. After the hot rolling with a 68% reduction and cold rolling with a 57% reduction, elongated grains in the main direction, alongside the equiaxed grains were observed [Figure 2.c)].

Figure 2.d) shows the microstructure of a processed specimen after recrystallization and stabilization, consisting of equiaxed recrystallized fine grains; at the grain boundaries, the presence of insoluble compounds based on Fe ( $\text{AlFeSi}$ ) and Mn ( $\text{Al}_6\text{Mn}$ ) can be identified. The 2024 aluminum alloy contains Mn, as the refining element, and Al-Mn pins at the grain boundaries at higher temperatures; these might have contributed to the microstructural stability observed at temperatures below 480°C. The average grain size at the center of the processing region was found to be about 5-8  $\mu\text{m}$ .

### 3.2. Superplastic behavior

Figure 3 is a plot of true stress versus true plastic strain for the samples tested at given strain rates at 460°C.

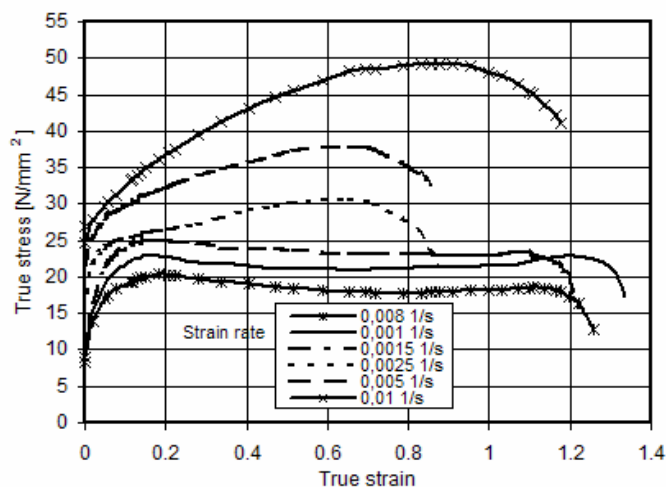


**Fig. 3.** True stress versus true strain at 460°C for samples of 2024 aluminum alloy thermomechanically processed.

As can be seen in Figure 3, the material revealed strain hardening regime at high strain rates ( $2.5 \times 10^{-3}$ ,  $5 \times 10^{-3}$  and  $1 \times 10^{-2} \text{ s}^{-1}$ ), followed by strain softening. At lower strain rates, low hardening or softening is observed and a straight zone where the true stress is approximately constant.

The strain rate can have a substantial effect on the true stress. Under conditions of deformation at high temperatures and low strain rates, the resulted curves are almost horizontal (perfectly plastic zone) due to diffusion, recovery and recrystallization mechanisms, having time to counterbalance strain-hardening effects [8]. At these strain rates, the superplastic behavior of 2024 aluminum alloy can be observed.

At high strain rates, there is no longer sufficient time for that to occur and stress increases as a function of strain.

Figure 4 presents ductility values plotted against temperatures, obtained for different strain rates ( $8 \times 10^{-4} \div 1 \times 10^{-2} \text{ s}^{-1}$ ). A maximum elongation of 269% was measured in the superplastic condition of  $480^\circ\text{C}$  and a  $5 \times 10^{-3} \text{ s}^{-1}$  strain rate, whereas at  $460^\circ\text{C}$ , values more than 200% were obtained at lower strain rates ( $8 \times 10^{-4} \div 1.5 \times 10^{-3} \text{ s}^{-1}$ ) (218%, 245.5% and 220.5% at  $8 \times 10^{-4} \text{ s}^{-1}$ ,  $1 \times 10^{-3} \text{ s}^{-1}$  and  $1.5 \times 10^{-3} \text{ s}^{-1}$  strain rates).

It may be mentioned that  $460^\circ\text{C}$  (at which superplastic behavior at the lowest strain rates is obtained), is lower than the conventional temperature ( $500^\circ\text{C}$ ) for superplasticity in aluminum alloys [1].

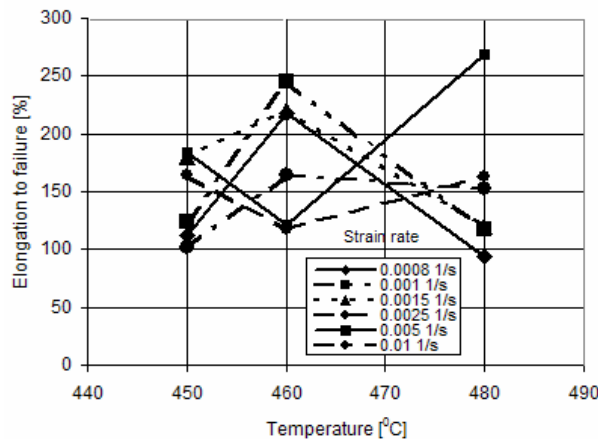


**Fig. 4.** Variation of elongation to failure with temperatures at different strain rates.

The strain rate sensitivity exponent,  $m$ , was determined by a computer program developed in C++ [7], during hot tensile tests, with constant strain rate and temperature for a given temperature, a given true strain (0.1) and a range of strain rates ( $8 \times 10^{-4} \div 1.5 \times 10^{-3} \text{ s}^{-1}$ ) and flow stress resulted from experimental tests

(Fig. 5). In general, the higher values of the strain rate sensitivity exponent at high temperatures are attributed to increased speed of heat of activated processes such as dislocation climb and grain boundary sliding.

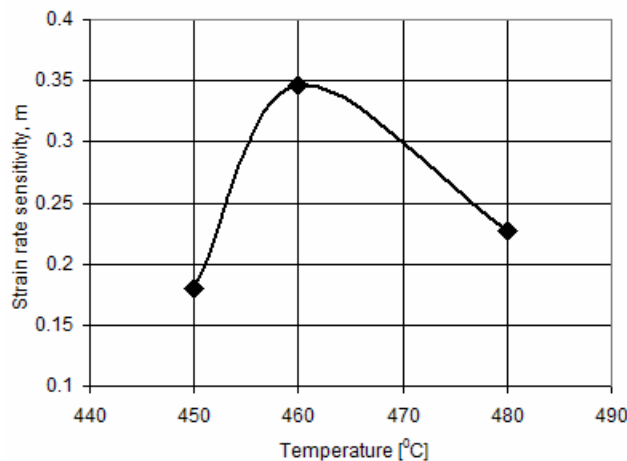


**Fig. 5.** Strain rate sensitivity exponent at different temperatures for 2024 aluminum alloy.

The value of the strain rate sensitivity exponent increases with temperature, but at a temperature of 460°C, where the alloy shows superplastic behavior, a value of  $m$  greater than at other temperatures is obtained, although still to the lower limit of the

requirement for the micrograin superplasticity ( $m > 0.3$ ) ( $m = 0.3462$ ).

Figure 6 shows hemispheres, obtained from circular membranes of fine grained 2024 aluminum alloy, that were free-bulged under low air pressure.



**Fig. 6.** Hemispheres obtained through free-bulging under low pressure.

#### 4. Conclusions

- Superplasticity can be achieved in a commercial 2024 aluminum alloy by thermomechanical processing.
- The maximum elongation of 269% was obtained at 480°C and a strain rate of  $5 \times 10^{-3} \text{ s}^{-1}$  in the thermomechanically processed alloy.
- Elongations higher than 200% were also achieved in tensile testing at 460°C (218%, 245.5% and 220.5% at strain rates of  $8 \times 10^{-4} \text{ s}^{-1}$ ,  $1 \times 10^{-3} \text{ s}^{-1}$  and  $1.5 \times 10^{-3} \text{ s}^{-1}$ ).
- An average grain size of  $5 \div 8 \mu\text{m}$  can be achieved by control of recrystallization.
- In 2024 aluminum alloy, the value of the strain rate sensitivity exponent to a true strain of 0.1 has the highest value - 0.3462 at 460°C and a strain rates range of  $8 \times 10^{-4} \div 1.5 \times 10^{-3} \text{ s}^{-1}$ , where the aluminum alloy shows superplastic behavior.
- By gas pressure blow forming tests, the possibility of obtaining hemispheres from 2024 aluminum alloy sheets, thermomechanically processed by hot rolling, cold rolling and recrystallization was demonstrated.

#### References

- [1]. Charit, I. and Mishra, R.S. - *High Strain Rate Superplasticity in a Commercial 2024 Al Alloy Via Friction Stir Processing*. In: Materials Science and Engineering A, volume 359, Issues 1-2, 2003, pp. 290-296.
- [2]. Perce, R. - *Sheet Metal Forming*, Institute of Physics Publishing, Philadelphia: Hilger, 1991, pp. 122-127.
- [3]. Pilling, J. and Ridley, N. - *Superplasticity in Crystalline Solids*. The Institute of Metals, London, 1989, pp. 3-8.
- [4]. Langdon, T.G., Wadsworth, J. - *Superplasticity in Advanced Materials*, The Japan Society for Research on Superplasticity, Osaka (Japan), 1991, p. 847.
- [5]. Langdon, T.G. - *Mechanisms of Superplastic Flow*. In: Superplasticity: 60 Years after Pearson, Edited by Norman Ridley, The Institute of Materials, London, 1995, pp. 9-13.
- [6]. Carrino, L., Giuliano, G. and Palmieri, C. - *On the Optimisation of Superplastic Forming Processes by the Finite-Element Method*. In: Journal of Materials Processing Technology, volumes 143-144, 2003, pp. 373-377.
- [7]. Rus A. L. - *Cercetari privind comportarea superplastica a materialelor metalice (Researches Concerning Superplastic Behaviour of Metallic Materials)* - Ph.D. Thesis - Technical University of Cluj-Napoca, 2006.
- [8]. Guillard, S. - *Workpiece Materials Database*. In: Metalworking: Bulk Forming, volume 14 A, ASM International, The Materials Information Society, 2005, pp. 651-659.